Detection of Deterioration of Three-phase Induction Motor using Vibration Signals

Adam Glowacz[1], Witold Glowacz[1], Jarosław Kozik[2], Krzysztof Piech[2], Miroslav Gutten[3], Wahyu Caesarendra[4], Hui Liu[5], Frantisek Brumercik[6], Muhammad Irfan[7], Z. Faizal Khan[8]

[1] AGH University of Science and Technology, Faculty of Electrical Engineering, Automatics, Computer Science and Biomedical Engineering, Department of Automatic Control and Robotics, Al. A. Mickiewicza 30, 30-059 Kraków, Poland, adglow@agh.edu.pl, wglowacz@agh.edu.pl
[2] AGH University of Science and Technology, Faculty of Electrical Engineering, Automatics, Computer Science and Biomedical Engineering, Department of Power Electronics and Energy Control Systems, Al. A. Mickiewicza 30, 30-059 Kraków, Poland, kozik@agh.edu.pl, kpiech@agh.edu.pl
[3] University of Zilina, Faculty of Electrical Engineering, 1, Univerzitna Str., 01026 Zilina, Slovakia, miroslav.gutten@fel.uniza.sk
[4] Faculty of Integrated Technologies, Universiti Brunei Darussalam, Jalan Tungku Link, Gadong BE1410, Brunei Darussalam, wahyu.caesarendra@ubd.edu.bn
[5] College of Quality and Safety Engineering, China Jiliang University, Hangzhou 310018, China, liuhui2003@126.com
[6] University of Zilina, Mechanical Engineering Faculty, Department of Desing and Machine Elements, 1 Univerzitna Str., 01026 Zilina, Slovakia, frantisek.brumercik@fstroj.uniza.sk
[7] Najran University, Electrical Engineering Department, Kingdom of Saudi Arabia, miditta@nu.edu.sa
[8] Shaqra University, College of Computing and Information Technology, Department of Computer Science, Kingdom of Saudi Arabia, faizalkhan@su.edu.sa

Nowadays detection of deterioration of electrical motors is an important topic of research. Vibration signals often carry diagnostic information of a motor. The authors proposed a setup for the analysis of vibration signals of three-phase induction motors. In this paper rotor fault diagnostic techniques of a three-phase induction motor (TPIM) were presented. The presented techniques used vibration signals and signal processing methods. The authors analyzed the recognition rate of vibration signal readings for 3 states of the TPIM: healthy TPIM, TPIM with 1 broken bar, and TPIM with 2 broken bars. In this paper the authors described a method of the feature extraction of vibration signals Method of Selection of Amplitudes of Frequencies – MSAF-12. Feature vectors were obtained using FFT, MSAF-12, and mean of vector sum. Three methods of classification were used: Nearest Neighbor (NN), Linear Discriminant Analysis (LDA), and Linear Support Vector Machine (LSVM). The obtained results of analyzed classifiers were in the range of 97.61 % – 100 %.

Keywords: signal processing, vibration signal, induction motor, deterioration, diagnosis.

1. INTRODUCTION

Induction motors are important parts of production lines and power plant generators. Each factory uses a lot of motors. Many thousands of motors break down every year. Degradation of motor is a process dependent on the operation time and construction of a motor. The damaged motor can stop the production line. It is reasonable to develop new techniques and diagnostic systems. To avoid an unexpected failure of the motor, operators use fault diagnosis systems and schedule needed repairs during maintenance shutdowns. It also allows operators to prevent production, money and time losses.

Diagnostic systems can measure different diagnostic signals such as: vibration, acoustic, electric current, voltage, infrared radiation, and axial flux. Axial flux was used for fault diagnosis of induction motors [1]-[4]. The analysis of axial flux has two advantages. The first is the lack of significant influence of the supply frequency and torque on the frequency spectrum. It can also detect asymmetry of the rotor and stator. The second advantage is that the analysis of the axial flux is faster than electrical current analysis. However, disadvantage is lack of measurement of the operational quantities, such as voltage or current. Moreover, there is a need to use different measuring coils. Measuring

coils depend on the size of the motor [1]. The possibility of using the axial flux for fault diagnosis of induction motors was presented [2]. Windings of the stator were analyzed using the axial flux and neural network [3]. The axial magnetic stray flux and the stator currents were analyzed and compared in the following paper [4].

The analysis based on electric signal is used for detection of mechanical (air-gap eccentricity, bearings, misalignment) and electrical faults (broken bars, shorted coils) of the motor. Physical access to the motor is not required because any change is detected by a transducer [5]. The MCSA (Motor current signal analysis) is a well-known method based on current monitoring [6]. The advantage of the analysis of current signal is that the signal is easy to process. The disadvantage of this analysis is that it is limited only to electrical motors. Moreover, some mechanical faults cannot be diagnosed by this technique, for example broken teeth of a sprocket. A novel approach of MCSA for fault detection of broken bars was presented in the paper [6]. Misalignment detection using MCSA was presented in the paper [7]. Measurement of the supply current and selected methods of diagnosis of induction motor bearings was presented in the paper [8]. The paper [9] presents fault diagnosis of induction motors using MCSA and EMD (Empirical Mode Decomposition).

Thermal analysis is also used for the detection of stator and rotor faults of induction motors (electrical faults). Electrical faults may cause losses. Losses increase the temperature of material. The generated heat can be measured by a thermal camera. Higher temperature causes shorter time of operation of the motor. The advantage of this analysis is non-invasive measurement. Thermal analysis gives us an image of the temperature distribution. It is also helpful to find anomaly of the motor. However, the technique based on thermal analysis can be used mostly for electrical faults [10]. In the paper, infrared thermography and MCSA are used for detection of three faults: bearing defects, unbalanced mass, and misalignment [10]. In the paper [11] the authors used thermal analysis for the detection of broken bars and faulty ring of squirrel-cage of a three-phase induction motor.

The analysis based on vibration signal is used for detection of mechanical and electrical faults of the motor [12]-[22]. Vibration analysis can recognize broken bars, shorted coils, a defective bearing, bent, misalignment. Vibration fault diagnosis allows engineers to evaluate the condition of the motor. First data acquisition captures multiple sine waves of vibration signals using accelerometer. It can be captured depending on the setup of the accelerometer (axes X, Y, Z). It is important to set the accelerometer correctly. Generated vibration signals can help us to detect the type of fault. However, it is difficult to localize the exact location of fault. Techniques and methods of vibration analysis of machines were developed [12]-[22]. The authors described a fault diagnosis method based on frequency-modulated empirical mode decomposition in the following paper [12]. A failure diagnostics approach was presented. The approach uses the manifold learning and swarm intelligence. Vibration data of the diesel engines were used for the analysis [13]. Vibration

signals of diesel engines were analyzed using the independent component analysis [14]. A review of the vibration-based condition monitoring of wind turbine was presented in the paper [15]. Next paper presents the method of fault diagnosis of in bevel gears. The author of the paper uses vibration signals and SVM (Support Vector Machine) for the analysis [16]. Vibration fault diagnosis of motorcycle (Honda Wave 100s model) was presented in the paper [17]. Vibration analysis of gearbox using iterative variational mode decomposition was presented in the following paper [18]. Condition monitoring of a gantry using vibration signals was presented in the paper [19]. A condition monitoring system using a vibration-electrical hybrid approach was described for induction motors [20]. Fault detection method of bearings of induction motors was developed in the paper [21]. A fault detection methodology using wavelet-based features of vibration signals was presented in the paper [22].

Acoustic analysis is also developed for fault diagnosis of induction motors. This type of analysis is often used for mechanical and electrical faults of rotating motors. Measurement can be done from a distance. The distance from an object affects the quality of the signal. Background noises cause distortion. Noisy samples with background noises cannot be used for proper recognition. Another problem is the selection of microphone. Capacity microphone is selected due to a larger frequency range. Fast Fourier transform (FFT)-based segmentation and acoustic fault identification algorithm were described in the paper [23]. Acoustic signals of gearbox acquired under various fault conditions were analyzed using continuous wavelet transform in the paper [24]. Acoustic signals of bearing defects using an improved one-against-all multiclass support vector machine (OAA-MCSVM) classifier were analyzed [25]. Acoustic signals of wind turbines were also analyzed [26]. The authors proposed an interesting iterative noise extraction and elimination method.

In the article detection techniques of deterioration of the TPIM were described, Fig.1.a), Fig.1.b), Fig.1.c). The authors proposed a setup of analysis of vibration signals of three-phase induction motors (Fig.2.). In this paper the authors implemented and used the method of feature extraction – MSAF-12. It was used for the analysis of vibration signals. Feature vectors were obtained using MSAF-12, FFT, and mean of vector sum. Vibration signal readings were used to compute feature vectors. The authors analyzed recognition rate of vibration signal readings for 3 states of the TPIM: healthy TPIM, TPIM with 1 broken bar, and TPIM with 2 broken bars. Three methods of classification were used: NN, LDA, and LSVM. The proposed techniques work well for analyzed three-phase induction motors. It can be used for detection of broken bars of electrical motors.

Development of the MSAF-12 method was motivated by an analysis of unknown acoustic signals. The MSAF-12 method is based on the fact that the acoustic signal can be recognized, if the proper frequency is extracted from the training set. Therefore, there is a need to have training vibration signals from a similar type of motor.
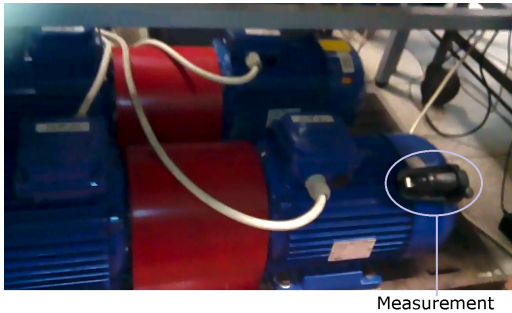
Fig.1.a) Three analyzed motors (healthy TPIM, TPIM with 1 broken bar, TPIM with 2 broken bars).
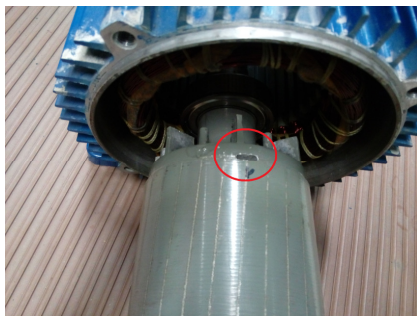

Fig.1.b) Rotor of TPIM with 1 broken bar.

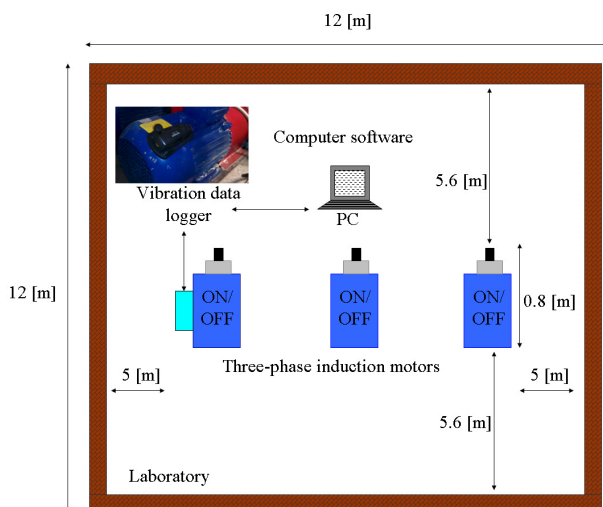Fig.1.c) Rotor of TPIM with 2 broken bars.

Fig.2. Experimental setup of analysis of vibration signals of three-phase induction motors.

The original contribution of the work includes:
- review of the literature related to vibration-based analysis of the motor,
- proper preparation of a database containing vibration signals of the motor,
- proposition of vibration-based diagnostic techniques,
- performing the analysis of captured vibration signals,
- drawing conclusions from the conducted analysis.

2. VIBRATION BASED ROTOR DIAGNOSTIC TECHNIQUES

The proposed vibration-based rotor diagnostic techniques consisted of signal processing methods (Fig.3.). Vibration data have been measured by a measuring device with an accelerometer. The authors used a low-cost device called Voltcraft DL-131G (vibration and acceleration USB data logger, 20 samples/second, 3-axis recording measuring range ±18G, G≈9.8 m/s^2) and computer software (Voltsoft Client and MATLAB). Other vibration, acceleration data loggers and computer software can be used for the proposed techniques. Next measured vibration data can be split (5-second sample – 5*20=100 measured values). The obtained samples (split vibration data) are used in the signal processing (windowing – size of a window = 100, FFT – 50 frequency components). There is also the possibility of using mean of *vector sum*. Next, the obtained frequency spectra are processed using the feature extraction method MSAF-12. The MSAF-12 method computed feature vectors (Fig.3.). The classification step consisted of patterns creation and testing (identification) process. In the testing process unknown test set was classified using training set and selected classifier. The method of feature extraction MSAF-12 was not used for the testing process, because all frequency components were computed by the MSAF-12 in the pattern creation. The computed feature vectors (frequency components) were processed by classification methods: NN, LDA, and LSVM.
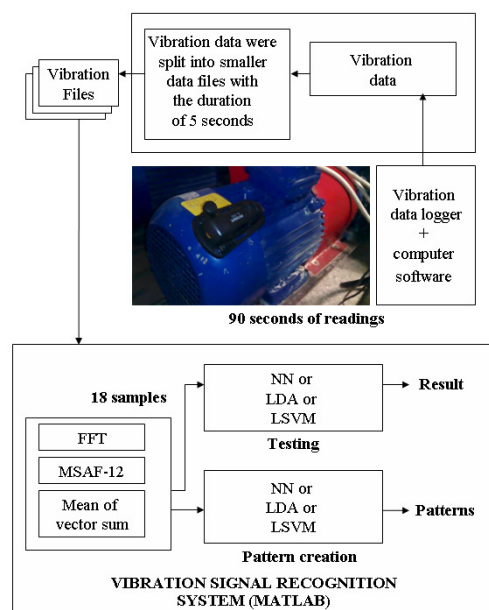

Fig.3. Proposed vibration-based rotor fault diagnostic techniques.

A. MSAF-12

The MSAF-12 extracts characteristic features of the vibration signal. It uses differences between frequency spectra of the vibration signal. The vibration signal is dependent on: faults, deterioration, rotor speed, material of motor, construction and size of the motor. The MSAF-12 has 5 steps:

1. Compute frequency spectrum for all samples of vibration signals. Vector **vhim**=[$vhim_1$, $vhim_2$, ..., $vhim_{50}$] represents the computed frequency spectrum of the vibration signal of the healthy TPIM. Vector **vpim**=[$vpim_1$, $vpim_2$, ..., $vpim_{50}$] defines the frequency spectrum of the vibration signal of the TPIM with 1 broken bar. Vector **vtim**=[$vtim_1$, $vtim_2$, ..., $vtim_{50}$] defines the frequency spectrum of the vibration signal of the TPIM with 2 broken bars.

2. Compute differences between computed frequency spectra: |**vhim - vpim**|, |**vhim - vtim**|, |**vpim - vtim**|.

3. Select 12 maximum frequency components for each computed difference: max_1|**vhim - vpim**|, ..., max_{12}|**vhim - vpim**|, max_1|**vhim - vtim**|, ..., max_{12}|**vhim - vtim**|, max_1|**vpim - vtim**|, ..., max_{12}|**vpim - vtim**|.

4. Find common frequencies (1-12) and find frequency components for each type of the vibration signal.

5. Form a feature vector.

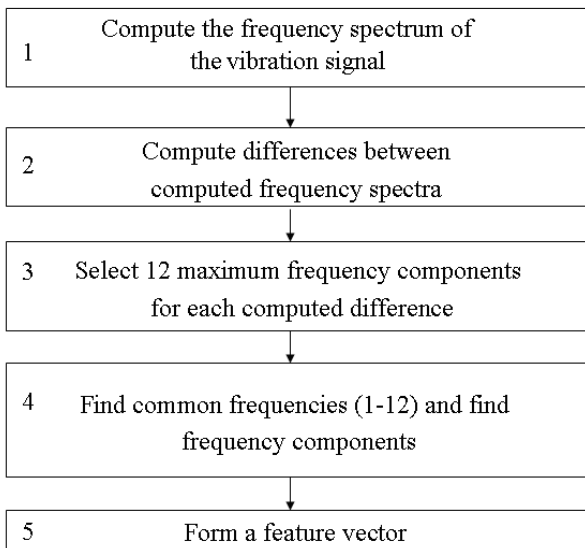Feature extraction method MSAF-12 is presented in Fig.4.

Fig.4. Feature extraction method MSAF-12.

The computed differences of frequency spectra of vibration signals |**vhim - vpim**|, |**vhim - vtim**|, |**vpim - vtim**| are presented in Fig.5. – Fig.7.

The MSAF-12 selects common frequency – 0.2 Hz. The obtained frequency component forms the feature vector. The MSAF-12 finds frequency components depending on differences between frequency coefficients of states of the TPIM. If we have a new motor (unknown acoustic signal for training samples, for example a train motor), then we need to analyze a new training set (new training set contains acoustic signals of induction motors and train motor). Selected frequency components depend on many parameters, for example construction of motor, material, rotor speed, place of measurement, etc. It can be used for other rotating motors.
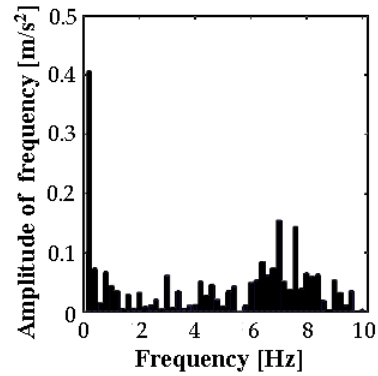

Fig.5. The computed difference (|vhim - vpim|).

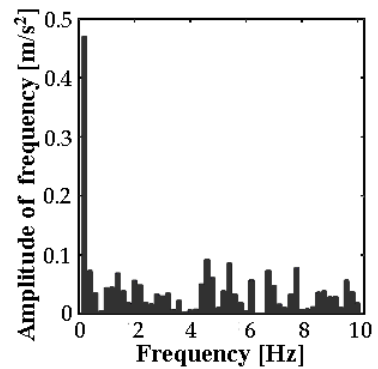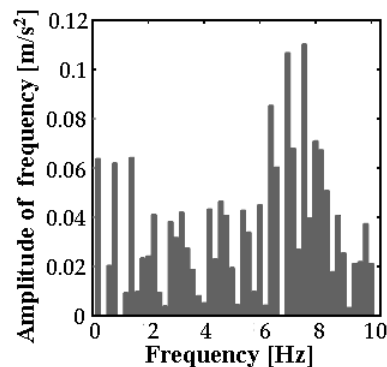Fig.6. The computed difference (|vhim - vtim|).

Fig.7. The computed difference (|vpim - vtim|).

The next step is the classification of feature vectors. The authors used the NN classifier [27], [28], [29], LDA [30], [31], and SVM [25], [32], [33]. However, other classifiers could be also used, for example neural network [34], [35].

B. Mean of vector sum

Another feature extraction method is *mean of vector sum*. Vibration and acceleration data logger measure: **X** value, **Y** value, **Z** value, and a value of *vector sum*. The value of *vector sum* is defined as (1):

$$vector\_sum = \sqrt[3]{|X|^3 + |Y|^3 + |Z|^3} \qquad (1)$$

where X, Y, Z – length of measured vectors.

Five-second sample has 100 values of *vector sum*. It is computed and presented in Table 1. for 18 samples of vibration signals. *Mean of vector sum* is expressed as (2):

$$Mean\_of\_vector\_sum = (\sum_{i=1}^{n} vector\_sum_i |)/n \qquad (2)$$

where *n*=100, for the presented analysis.

It can be noticed that the value of *Mean of vector sum* for the healthy TPIM was in the range 1.1878–1.2188 [m/s²]. The value of *Mean of vector sum* for the TPIM with 1 broken bar was in the range 1.3839–1.4186 [m/s²]. The value of *Mean of vector sum* for the TPIM with 2 broken bars was in the range 1.4505–1.5165 [m/s²].

Table 1. Mean of vector sum of 18 samples
of vibration signals.

Mean of vector sum [m/s²]		
healthy TPIM	TPIM with 1 broken bar	TPIM with 2 broken bars
1.2188	1.4186	1.5165
1.2152	1.4022	1.4505
1.1917	1.3872	1.4872
1.1878	1.4050	1.4829
1.1970	1.4086	1.4685
1.1914	1.3839	1.4925

C. NN classifier

The NN (Nearest Neighbor) classifier is discussed by scientists all over the world [27] – [29], [36]. The classifier is useful for pattern recognition: diagnostic signals, temperature, images, measured data, text. It is a supervised classifier. It takes labels into consideration. The method uses training set and test set. Test vector is compared with training vectors using selected distance function. All distances are computed and usually one computed distance is the nearest distance. Next test vector is recognized using label of class and the computed nearest distance. The Nearest Neighbor method classifies test vectors using: Chebyshev, Manhattan, Euclidean, Minkowski, or the cosine distance. In the analysis the Manhattan distance (3) is applied for the classification of feature vectors. It is expressed as:

$$D(\mathbf{vhim}, \mathbf{vpim}) = \sum_{i=1}^{j} (vhim_i - vpim_i) | \qquad (3)$$

where test feature vector is defined as **vhim**=[$vhim_1$] and training feature vector is expressed as **vpim** =[$vpim_1$], *j* − number of features, *i*=1,..., *j*. The Manhattan distance was computed for all test and training feature vectors.

The authors computed total efficiency of vibration signal recognition (see formula 5) using the Manhattan distance. However, similar results (Table 2.) can be achieved by the Euclidean, Minkowski, or cosine distance. Description of the NN can be found in the following literature [27]-[29], [36].

D. LDA classifier

The Linear Discriminant Analysis (LDA) was developed in 1936 by Fisher. The LDA reduces a dimensionality of data. It is used for pattern classification applications. The original LDA was developed for a 2-class problem. Next it was described for multi-class problem by Rao in 1948. The goal of classifier is to project dataset n-dimensional vectors onto a smaller subspace k (where k≤n−1). It is a supervised classifier. It takes labels into consideration. The LDA is performed in 5 steps:

1. Compute *d*-dimensional mean vectors (**mv**$_i$).
2. Compute between-class matrix (M_B) and within-class scatter matrix (M_W). M_B is the distance between **mv**$_i$ of different classes. It is computed to separate different classes. M_W is the distance between **mv**$_i$ and sample of each class.
3. Compute eigenvectors (**ev**$_1$, **ev**$_2$, ..., **ev**$_d$) and eigenvalues (**λv**$_1$, **λv**$_2$, ..., **λv**$_d$).
4. Select linear discriminants for the new feature subspace. Form an eigenvector matrix **EM**.
5. Use the eigenvector matrix **EM** to transform the vectors onto the new lower dimensional space. Maximize M_B and minimize M_W.

Description of the LDA classifier can be found in the following literature [30], [31].

E. LSVM classifier

The Linear Support Vector Machine (LSVM) is a linear model for classification of data. It is described in the literature [25], [32], [33]. The classifier is useful for recognizing: images, measured data, and text. The LSVM is used for linearly separable data. The method classifies vectors by finding the best hyperplane. The hyperplane separates training feature vectors between two classes. The LSVM computes the maximum distance between the two analyzed classes. It was necessary for proper classification of feature vectors [25], [32], [33].

Feature vectors are labeled as -1 or 1. The label of feature vector depends on the computed hyperplane. Moreover, there are also two additional hyperplanes. These hyperplanes are parallel to the separating hyperplane. Some of the vectors are the closest to the separating hyperplane. The closest training feature vectors are cut through by additional hyperplanes. These training feature vectors are called "support vectors".

Description of the LSVM can be found in the following literature [25], [32], [33].

3. ANALYSIS OF VIBRATION SIGNALS

The analysis of vibration signals was conducted on one motor at a time (3 motors in total). The authors studied 1 healthy motor, one motor with 1 broken bar, and 1 motor with 2 broken bars. The analyzed motors operated under open loop control. The parameters of the analyzed machines are shown below: $N_m = 1425$ rpm, $I_{NM} = 8.4/4.8$ A (Δ/Y), $P_m = 2200$ W, $\eta = 82$ %, where N_m – rotor speed, I_{NM} – nominal stator current, P_m – motor power, η – energy conversion efficiency.

The authors analyzed vibration signals of 3 states of the TPIM. In the analysis the authors measured signals from 1 electric motor simultaneously (healthy TPIM (Fig.8.), TPIM with 1 broken bar (Fig.9.a), Fig.9.b)), TPIM with 2 broken bars (Fig.10.).
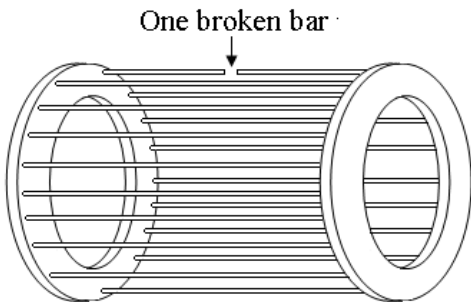

Fig.8. Healthy TPIM.

Fig.9.a) Scheme of squirrel cage of the TPIM with one broken bar.

Fig.9.b) Squirrel cage of the TPIM with one broken bar.
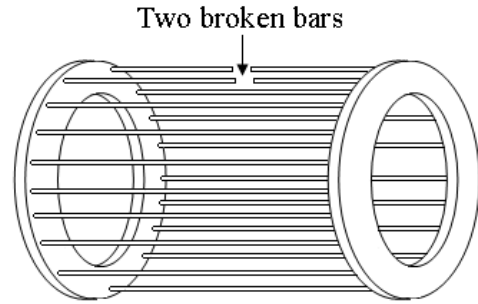

Fig.10.a) Scheme of squirrel cage of the TPIM with two broken bars.
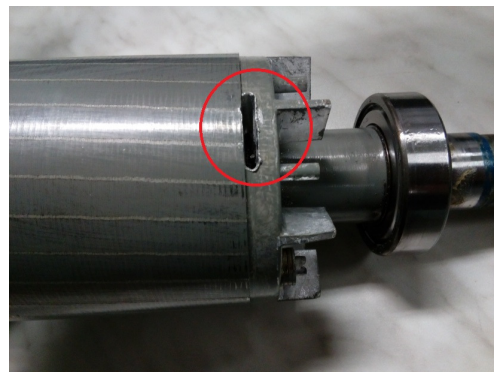

Fig.10.b) Squirrel cage of the TPIM with two broken bars.

Training set consisted of 18 training samples of vibration signals (each sample has 5 seconds of vibration signal – 100 measured values). Test set consisted of 504 test samples of vibration signals. Training and test samples of vibration signals were computed by proposed diagnostic techniques (Fig.3.). To evaluate the results, the authors used efficiency of vibration signal recognition. It is defined as (4):

$$E_{VSR} = \frac{N_{TSV}}{N_{ASV}} \cdot 100\%$$ (4)

where: N_{TSV} – number of vibration test samples recognized properly, N_{ASV} – number of vibration test samples in the training set, E_{VSR} – efficiency of vibration signal recognition.

To evaluate 3 states of the motor, the authors used total efficiency of vibration signal recognition. It is expressed as (5):

$$TE_{VSR} = \frac{E_{VSR1} + E_{VSR2} + E_{VSR3}}{3}$$ (5)

where: E_{VSR1} – E_{VSR} of the healthy TPIM, E_{VSR2} – E_{VSR} of the TPIM with 1 broken bar, E_{VSR3} – E_{VSR} of the TPIM with 2 broken bars, TE_{VSR} – total efficiency of vibration signal recognition.

The computed results are shown in Table 2. - Table 6. In Table 2., the authors present the computed results of recognition of vibration signals. The MSAF-12 and the NN classifier were used.

Table 2. The computed results of recognition of vibration signals. The MSAF-12 and the NN classifier were used.

Type of the vibration signal	E_{VSR} [%]
healthy TPIM	100
TPIM with 1 broken bar	100
TPIM with 2 broken bars	100
TE_{VSR}	100

In Table 3., the authors show the computed results of recognition of vibration signals. The MSAF-12 and the LDA classifier were used.

Table 3. The computed results of recognition of vibration signals. The MSAF-12 and the LDA classifier were used.

Type of the vibration signal	E_{VSR} [%]
healthy TPIM	100
TPIM with 1 broken bar	100
TPIM with 2 broken bars	100
TE_{VSR}	100

In Table 4., the authors present the computed results of recognition of vibration signals. The MSAF-12 and the LSVM classifier were used.

Table 4. The computed results of recognition of vibration signals. The MSAF-12 and the LSVM classifier were used.

Type of the vibration signal	E_{VSR} [%]
healthy TPIM	100
TPIM with 1 broken bar	100
TPIM with 2 broken bars	100
TE_{VSR}	100

In Table 5., the authors show the computed results of recognition of vibration signals. The FFT and the NN classifier were used.

Table 5. The computed results of recognition of vibration signals. The FFT and the NN classifier were used.

Type of the vibration signal	E_{VSR} [%]
healthy TPIM	100
TPIM with 1 broken bar	100
TPIM with 2 broken bars	92.85
TE_{VSR}	97.61

In Table 6., the authors present the computed results of recognition of vibration signals. The mean of vector sum and the NN classifier were used.

Table 6. The computed results of recognition of vibration signals. The mean of vector sum and the NN classifier were used.

Type of the vibration signal	E_{VSR} [%]
healthy TPIM	100
TPIM with 1 broken bar	100
TPIM with 2 broken bars	100
TE_{VSR}	100

The obtained results of analyzed classifiers were in the range of 97.61 % – 100 % (TE_{VSR} was in the range of 97.61 % – 100 %). The MSAF-12 and *mean of vector sum* had TE_{VSR}=100 %. The MSAF-12 selected specific frequency components based on differences of frequency spectra. *Mean of vector sum* analyzed 1 value – mean of 100 measured values. *Mean of vector sum* can only be used for limited faults. If amplitudes of vibration signals are similar it will not work properly. The MSAF-12 is based on the FFT spectrum and it can work properly in this case.

4. CONCLUSIONS

This paper describes diagnostic techniques of rotor of the TPIM. The proposed techniques were based on vibration signals. The authors analyzed vibration signals for 3 states of the TPIM. The authors studied 1 healthy motor, one motor with 1 broken bar, and 1 motor with 2 broken bars (3 motors in total). The authors developed and used the MSAF-12 method. Feature vectors were obtained using MSAF-12, FFT, and mean of vector sum.

Next, 3 methods of classification were used: NN, LDA, and LSVM. The computed results of the mentioned classifiers were comparable with results obtained by other diagnostic methods (TE_{VSR} was equal to 100 % for the MSAF-12). The described diagnostic techniques are inexpensive. Vibration and acceleration data loggers cost about $100. The cost of computer is in the range of $250-300. As presented in the results section, presented techniques work well for detection of deterioration. The article showed that vibration signal has diagnostic information. The proposed techniques can be also used to detect faults of rotating electrical motors – bearings faults, broken sprocket teeth, broken gears.

This study calls for future research of proposed vibration-based techniques. Future techniques will be extended by analysis of acoustic, electrical, and thermal signals. Other faults, operating parameters of TPIM will be analyzed and used for industry.

REFERENCES

[1] Tulicki, J., Petryna, J., Sulowicz, M. (2016). Fault diagnosis of induction motors in selected working conditions based on axial flux signals. *Technical Trasactions*, Electrical Engineering Issue 3-E, 99-113. DOI: 10.4467/2353737XCT.16.269.6068.

[2]   Ewert, P. (2017). Use of axial flux in the detection of electrical faults in induction motors. In *International Symposium on Electrical Machines (SME)*. IEEE, DOI: 10.1109/ISEM.2017.7993571.

[3]   Pietrowski, W. (2011). Application of Radial Basis Neural Network to diagnostics of induction motor stator faults using axial flux. *Przeglad Elektrotechniczny*, 87 (6), 190-192.

[4]   Fulnecek, J., Misak, S. (2018). Stator current and axial magnetic flux analysis of induction motor. In *International Conference on Diagnostics in Electrical Engineering (Diagnostika)*. IEEE, DOI: 10.1109/DIAGNOSTIKA.2018.8526025.

[5]   Calis, H. (2014). Vibration and motor current analysis of induction motors to diagnose mechanical faults. *Journal of Measurements in Engineering*, 2 (4), 190-198.

[6]   Garcia-Bracamonte, J.E., Ramirez-Cortes, J.M., Rangel-Magdaleno, J.D., Gomez-Gil, P., Peregrina-Barreto, H., Alarcon-Aquino, V. (2019). An approach on MCSA-based fault detection using independent component analysis and neural networks. *IEEE Transactions on Instrumentation and Measurement*, 68 (5), 1353-1361. DOI: 10.1109/TIM.2019.2900143.

[7]   Verucchi, C., Bossio, J., Bossio, G., Acosta, G. (2016). Misalignment detection in induction motors with flexible coupling by means of estimated torque analysis and MCSA. *Mechanical Systems and Signal Processing*, 80, 570-581. DOI: 10.1016/j.ymssp.2016.04.035.

[8]   Ciszewski, T., Swedrowski, L., Gelman, L. (2015). Induction motor bearings diagnostic using MCSA and normalized tripple covariance. In *IEEE 10th International Symposium on Diagnostics for Electrical Machines, Power Electronics and Drives (SDEMPED)*. IEEE, 333-337. DOI: 10.1109/DEMPED.2015.7303711.

[9]   Valles-Novo, R., Rangel-Magdaleno, J., Ramirez-Cortes, J., Peregrina-Barreto, H., Morales-Caporal, R. (2014). Broken bar detection on squirrel cage induction motors with MCSA and EMD. In *IEEE International Instrumentation and Measurement Technology Conference (I2MTC) Proceedings*. IEEE, 993-998. DOI: 10.1109/I2MTC.2014.6860892.

[10] Garcia-Ramirez, A.G., Morales-Hernandez, L.A., Osornio-Rios, R.A., Garcia-Perez, A., Romero-Troncoso, R.J. (2014). Thermographic technique as a complement for MCSA in induction motor fault detection. In *International Conference on Electrical Machines (ICEM)*. IEEE, 1940-1945. DOI: 10.1109/ICELMACH.2014.6960449.

[11] Glowacz, A., Glowacz, Z. (2017). Diagnosis of the three-phase induction motor using thermal imaging. *Infrared Physics & Technology*, 81, 7-16. DOI: 10.1016/j.infrared.2016.12.003.

[12] Zhang, C., Peng, Z.X., Chen, S., Li, Z.X., Wang, J.G. (2018). A gearbox fault diagnosis method based on frequency-modulated empirical mode decomposition and support vector machine. *Proceedings of the Institution of Mechanical Engineers, Part C: Journal of Mechanical Engineering Science*, 232 (2), 369-380. DOI: 10.1177/0954406216677102.

[13] Li, Z.X., Jiang, Y., Duan, Z.H., Peng, Z.X. (2018). A new swarm intelligence optimized multiclass multi-kernel relevant vector machine: An experimental analysis in failure diagnostics of diesel engines. *Structural Health Monitoring*, 17 (6), 1503-1519. DOI: 10.1177/1475921717746735.

[14] Xi, W.K., Li, Z.X., Tian, Z., Duan, Z.H. (2018). A feature extraction and visualization method for fault detection of marine diesel engines. *Measurement*, 116, 429-437. DOI: 10.1016/j.measurement.2017.11.035.

[15] Wang, T.Y., Han, Q.K., Chu, F.L., Feng, Z.P. (2019). Vibration based condition monitoring and fault diagnosis of wind turbine planetary gearbox: A review. *Mechanical Systems and Signal Processing*, 126, 662-685. DOI: 10.1016/j.ymssp.2019.02.051.

[16] Ebrahimi, E. (2019). A method based on support vector machine and vibration analysis for fault detection in bevel gears (Case study: Differential). *Insight*, 61 (5), 279-286. DOI: 10.1784/insi.2019.61.5.279.

[17] Chomphan, S. (2019). Vibration signal analysis of a motorcycle. *International Journal of GEOMATE*, 16 (56), 27-32. DOI: 10.21660/2019.56.4549.

[18] Isham, M.F., Leong, M.S., Heel, L.M., Ahmad, Z.A.B. Iterative variational mode decomposition and extreme learning machine for gearbox diagnosis based on vibration signals. *Journal of Mechanical Engineering and Sciences*, 13 (1), 4477-4492. DOI: 10.15282/jmes.13.1.2019.10.0380.

[19] Sikora, M., Szczyrba, K., Wrobel, L., Michalak, M. (2019). Monitoring and maintenance of a gantry based on a wireless system for measurement and analysis of the vibration level. *Eksploatacja i Niezawodnosc (Maintenance and Reliability)*, 21 (2), 341-350. DOI: 10.17531/ein.2019.2.19.

[20] Chang, H.C., Jheng, Y.M., Kuo, C.C., Hsueh, Y.M. (2019). Induction motors condition monitoring system with fault diagnosis using a hybrid approach. *Energies*, 12 (8). DOI: 10.3390/en12081471.

[21] Suh, S., Lee, H., Jo, J., Lukowicz, P., Lee, Y.O. (2019). Generative oversampling method for imbalanced data on bearing fault detection and diagnosis. *Applied Sciences-Basel*, 9 (4). DOI: 10.3390/app9040746.

[22] Gangsar, P., Tiwari, R. (2019). Diagnostics of mechanical and electrical faults in induction motors using wavelet-based features of vibration and current through support vector machine algorithms for various operating conditions. *Journal of the Brazilian Society of Mechanical Sciences and Engineering*, 41 (2). DOI: 10.1007/s40430-019-1574-5.

[23] Gowid, S., Dixon, R., Ghani, S., Shokry, A. (2019). Robustness analysis of the FFT-based segmentation, feature selection and machine fault identification algorithm. *Insight*, 61 (5), 271-278. DOI: 10.1784/insi.2019.61.5.271.

[24] Parey, A., Singh, A. (2019). Gearbox fault diagnosis using acoustic signals, continuous wavelet transform and adaptive neuro-fuzzy inference system. *Applied Acoustics*, 147, 133-140. DOI: 10.1016/j.apacoust.2018.10.013.

[25] Islam, M.M.M., Kim, J.M. (2019). Reliable multiple combined fault diagnosis of bearings using heterogeneous feature models and multiclass support vector Machines. *Reliability Engineering & System Safety*, 184, 55-66. DOI: 10.1016/j.ress.2018.02.012.

[26] Fushun, L., Shujian, G., Huawei, H., Zhe, T., Peng, L. (2019). Interference reduction of high-energy noise for modal parameter identification of offshore wind turbines based on iterative signal extraction. *Ocean Engineering*, 183, 372–383. DOI: 10.1016/j.oceaneng.2019.05.009.

[27] Hasan, M.J., Kim, J.M. (2019). Fault detection of a spherical tank using a genetic algorithm-based hybrid feature pool and k-nearest neighbor algorithm. *Energies*, 12 (6). DOI: 10.3390/en12060991.

[28] Xiong, J.B., Zhang, Q.H., Peng, Z.P., Sun, G.X., Xu, W.C., Wang, Q. (2015). A diagnosis method for rotation machinery faults based on dimensionless indexes combined with k-nearest neighbor algorithm. *Mathematical Problems in Engineering*. DOI: 10.1155/2015/563954.

[29] Zhou, Y.Q., Sun, B.T., Li F.P., Song, W.L. (2015). NC machine tools fault diagnosis based on kernel PCA and k-nearest neighbor using vibration signals. *Shock and Vibration*. DOI: 10.1155/2015/139217.

[30] Yadav, A., Swetapadma, A. (2015). A novel transmission line relaying scheme for fault detection and classification using wavelet transform and linear discriminant analysis. *Ain Shams Engineering Journal*, 6, 199-209. DOI: 10.1016/j.asej.2014.10.005.

[31] Haddad, R.Z., Strangas, E.G. (2016). On the accuracy of fault detection and separation in permanent magnet synchronous machines using MCSA/MVSA and LDA. *IEEE Transactions on Energy Conversion*, 31, 924-934. DOI: 10.1109/TEC.2016.2558183.

[32] Fu, W.L., Tan, J.W., Xu, Y.H., Wang, K., Chen, T. (2019). Fault diagnosis for rolling bearings based on fine-sorted dispersion entropy and SVM optimized with mutation SCA-PSO. *Entropy*, 21 (4). DOI: 10.3390/e21040404.

[33] Jiang, Q.Y., Chang, F.L. (2019), A novel rolling-element bearing faults classification method combines lower-order moment spectra and support vector machine. *Journal of Mechanical Science and Technology*, 33 (4), 1535-1543. DOI: 10.1007/s12206-019-0305-2.

[34] Gajewski, J., Valis, D. (2017). The determination of combustion engine condition and reliability using oil analysis by MLP and RBF neural networks. *Tribology International*, 115, 557-572. DOI: 10.1016/j.triboint.2017.06.032.

[35] Hu, Z.B., Su, J., Jotsov, V., Kochan, O., Mykyichuk, M., Kochan, R., Sasiuk, T. (2016). Data science applications to improve accuracy of thermocouples. In *IEEE 8th International Conference on Intelligent Systems (IS)*. IEEE, 180-188. DOI: 10.1109/IS.2016.7737419.

[36] Glowacz, A., Glowacz, Z. (2016). Recognition of images of finger skin with application of histogram, image filtration and K-NN classifier. *Biocybernetics and Biomedical Engineering*, 36, 95-101. DOI: 10.1016/j.bbe.2015.12.005.